A wavelength-tunable fiber-coupled source of narrowband entangled photons

Alessandro Fedrizzi[1]**, Thomas Herbst**[1]**, Andreas Poppe**[2]**, Thomas Jennewein**[1] **and Anton Zeilinger**[1,2]

[1]*Institute for Quantum Optics and Quantum Information, Austrian Academy of Sciences, Boltzmanngasse 3, 1090 Wien, Austria*
[2]*Quantum Optics, Quantum Nanophysics and Quantum Information, Faculty of Physics, University of Vienna, Boltzmanngasse 5, 1090 Vienna, Austria*

zeilinger-office@univie.ac.at

Abstract: We demonstrate a wavelength-tunable, fiber-coupled source of polarization-entangled photons with extremely high spectral brightness and quality of entanglement. Using a 25 mm PPKTP crystal inside a polarization Sagnac interferometer we detect a spectral brightness of 273000 pairs $(\text{s mW nm})^{-1}$, a factor of 28 better than comparable previous sources while state tomography showed the two-photon state to have a tangle of $T = 0.987$. This improvement was achieved by use of a long crystal, careful selection of focusing parameters and single-mode fiber coupling. We demonstrate that, due to the particular geometry of the setup, the signal and idler wavelengths can be tuned over a wide range without loss of entanglement.

© 2007 Optical Society of America

OCIS codes: (270.0270) Quantum Optics; (190.4410) Nonlinear Optics, parametric processes;

References and links

1. A. K. Ekert, "Quantum cryptography based on Bells theorem," Phys. Rev. Lett. **67**, 661-663 (1991).
2. T. Jennewein, C. Simon, G. Weihs, H. Weinurter, and A. Zeilinger, "Quantum cryptography with entangled photons," Phys. Rev. Lett. **84**, 4729-4732 (2000).
3. C. H. Bennett, G. Brassard, C. Crépeau, R. Jozsa, A. Peres, and W. K. Wootters, "Teleporting an unknown quantum state via dual classical and Einstein-Podolsky-Rosen channels," Phys. Rev. Lett. **70**, 1895-1899 (1993).
4. D. Bouwmeester, J. W. Pan, K. Mattle, M. Eibl, H. Weinfurter, and A. Zeilinger, "Experimental quantum teleportation," Nature (London) **390**, 575-579 (1997).
5. E. Knill, R. Laflamme, and G. J. Milburn, "A scheme for efficient quantum computation with linear optics," Nature (London) **409**, 46-52 (2001).
6. P. G. Kwiat, K. Mattle, H. Weinfurter, A. Zeilinger, A. V. Sergienko, and Y. Shih, "New high-intensity source of polarization-entangled photon pairs," Phys. Rev. Lett. **75**, 4337-4341 (1995).
7. M. Pelton, P. Marsden, D. Ljunggren, M. Tengner, A. Karlsson, A. Fragemann, C. Canalias, and F. Laurell, "Bright, single-spatial-mode source of frequency non-degenerate, polarization-entangled photon pairs using periodically poled KTP," Opt. Express **12**, 3573-3580 (2004).
8. F. König, E. J. Mason, F. N. C. Wong, and M. A. Albota, "Efficient and spectrally bright source of polarization-entangled photons," Phys. Rev. A **71**, 033805 (2005).
9. H. Hübel, M. R. Vanner, T. Lederer, B. Blauensteiner, T. Lorünser, A. Poppe, and A. Zeilinger, "High-fidelity transmission of polarization encoded qubits from an entangled source over 100 km of fiber," Opt. Express **15**, 7853-7862 (2007).
10. C. E. Kuklewicz, M. Fiorentino, G. Messin, F. N. C. Wong, and J. H. Shapiro, "High-flux source of polarization-entangled photons from a periodically poled KTiOPO$_4$ parametric down-converter," Phys. Rev. A **69**, 013807 (2004).
11. P. G. Kwiat, P. H. Eberhard, A. M. Steinberg, and R. Y. Chiao, "Proposal for a loophole-free Bell inequality experiment," Phys. Rev. A **49**, 3209-3220 (2004).

12. M. Fiorentino, G. Messin, C. E. Kuklewicz, F. N. C. Wong, and J. H. Shapiro, "Generation of ultrabright tunable polarization entanglement without spatial, spectral, or temporal constraints," Phys. Rev. A **69**, 041801 (2004).

13. B. S. Shi and A. Tomita, "Generation of a pulsed polarization entangled photon pair using a Sagnac interferometer," Phys. Rev. A **69**, 013803 (2004).

14. T. Kim, M. Fiorentino, and F. N. C. Wong, "Phase-stable source of polarization-entangled photons using a polarization Sagnac interferometer," Phys. Rev. A **73**, 012316 (2006).

15. F. N. C. Wong, J. H. Shapiro, and T. Kim, "Efficient generation of polarization-entangled photons in a nonlinear crystal," Laser Physics, **16**, 1517-1524, (2006).

16. J. Fan and A. Migdall, "A broadband high spectral brightness fiber-based two-photon source," Opt. Express **15**, 2915-2920 (2007).

17. C. Liang, K. F. Lee, M. Medic, P. Kumar, R. H. Hadfield, and S. W. Nam, "Characterization of fiber-generated entangled photon pairs with superconducting single-photon detectors," Opt. Express **15**, 1322-1327, (2007).

18. S. M. Spillane, M. Fiorentino, and R. G. Beausoleil, "Spontaneous parametric down conversion in a nanophotonic waveguide," Opt. Express **15**, 8770-8780, (2007).

19. S. Gröblacher, T. Paterek, R. Kaltenbaek, C. Brukner, M. Zukowski, M. Aspelmeyer, and A. Zeilinger, "An experimental test of non-local realism," Nature (London) **446**, 871-875, (2007).

20. T. Paterek, A. Fedrizzi, S. Gröblacher, T. Jennewein, M. Zukowski, M. Aspelmeyer, and A. Zeilinger, "Experimental test of non-local realistic theories without the rotational symmetry assumption," arXiv:0708.0813v1 [quant-ph]

21. K. J. Resch, M. Lindenthal, B. Blauensteiner, H. R. Boehm, A. Fedrizzi, C. Kurtsiefer, A. Poppe, T. Schmitt-Manderbach, M. Taraba, R. Ursin, P. Walther, H. Weier, H. Weinfurter, and A. Zeilinger, "Distributing entanglement and single photons through an intra-city, free-space quantum channel," Opt. Express **13**, 1, 202-209 (2005).

22. C. Z. Peng, T. Yang, X. H. Bao, J. Zhang, X. M. Jin, F. Y. Feng, B. Yang, J. Yang, J. Yin, Q. Zhang, N. Li, B. L. Tian, and J. W. Pan, "Experimental free-space distribution of entangled photon pairs over 13km: towards satellite-based global quantum communication," Phys. Rev. Lett. **94**, 150501 (2005).

23. R. Ursin, F. Tiefenbacher, T. Schmitt-Manderbach, H. Weier, T. Scheidl, M. Lindenthal, B. Blauensteiner, T. Jennewein, J. Perdigues, P. Trojek, B. Ömer, M. Fürst, M. Meyenburg, J. Rarity, Z. Sodnik, C. Barbieri, H. Weinfurter, and A. Zeilinger, "Entanglement-based quantum communication over 144km," Nature Physics **3**, 481-486 (2007).

24. D. N. Matsukevich and A. Kuzmich, "Quantum state transfer between matter and light," Science **306**, 663-666 (2004).

25. B. Julsgaard, J. Sherson, I. Cirac, J. Fiurasek, and E. S. Polzik, "Experimental demonstration of quantum memory for light," Nature (London) **432**, 482-486 (2004).

26. C. Kurtsiefer, M. Oberparleitner, and H. Weinfurter, "High-efficiency entangled photon pair collection in type-II parametric fluorescence," Phys. Rev. A **64**, 023802 (2001).

27. F. A. Bovino, P. Varisco, M. A. Colla, G. Castagnoli, G. Di Giuseppe, and A. V. Sergienko, "Effective fiber-coupling of entangled photons for quantum communication," Opt. Commun. **227**, 343-348 (2003).

28. D. Ljunggren and M. Tengner, "Optimal focusing for maximal collection of entangled narrow-band photon pairs into single-mode fibers," Phys. Rev. A **72**, 062301 (2005).

29. M. H. Rubin, D. N. Klyshko, Y. H. Shi, and A. V. Sergienko, "Theory of two-photon entanglement in Type-II optical parametric down-conversion," Phys. Rev. A **50**, 5122-5233 (1994).

30. D. F. V. James, P. G. Kwiat, W. J. Munro, and A. G. White, "Measurement of qubits," Phys. Rev. A **64**, 052312 (2001).

31. V. Coffman, J. Kundu, and W. K. Wootters, "Distributed entanglement," Phys. Rev. A **61**, 052306 (2000).

32. K. Kato and E. Takaoka, "Sellmeier and thermo-optic formulas for KTP," Appl. Opt. **41**, 50405044 (2002).

33. S. Emanueli and A. Arie, "Temperature-dependent dispersion equations for KTiOPO4 and KTiOAsO4," Appl. Opt. **42**, 6661-6665, (2003).

34. M. Fiorentino, C. E. Kuklewicz, and F. Wong, "Source of polarization entanglement in a single periodically poled KTiOPO$_4$ crystal with overlapping emission cones," Opt. Express **13**, 1, 127-135 (2005).

1. Introduction

Sources for photonic entanglement form an integral part of quantum optics experiments and quantum information protocols like quantum key distribution [1,2], quantum teleportation [3,4] and quantum computing [5]. To date the most successful method of creating polarization entangled photon pairs is spontaneous parametric downconversion (SPDC) in nonlinear crystals. In the first practical and efficient scheme, orthogonally polarized photon pairs were created in a Type-II BBO bulk crystal and emitted along intersecting cones [6]. Since then nonlinear optics has advanced; Periodic poling of nonlinear crystals considerably relaxes the phasematching

conditions for SPDC and allows to fully exploit the material's nonlinear properties. These crystals are best employed in collinear configuration, where a much bigger fraction of the created photons can be entangled than in the conelike geometry of [6], thus leading to downconversion sources of higher spectral brightness. This increase comes at the cost of a new problem though, the need to spatially separate the collinear downconversion modes.

When the downconverted photons are created at substantially different wavelengths, they can be separated by dichroic mirrors, and several demonstrations of this have reported high spectral brightness [7–9]. For many applications, however, wavelength-degenerate photons are preferable. The first attempt to build a source based on periodically poled $KTiOPO_4$ (PPKTP) and collinear beam propagation used a simple beamsplitter to separate the output modes, at the cost of an unwanted 50% loss in the coincidences [10]. A more effective method, originally proposed in [11], is to interferometrically combine the outputs of two downconverters on a polarizing beamsplitter. The authors of [12] implemented this idea, using one bidirectionally pumped PPKTP crystal in a folded Mach-Zehnder interferometer. The spectral brightness of this source reached 4000 pairs$(s\,mW\,nm)^{-1}$, but the Mach-Zehnder interferometer was sensitive to vibrations and even with active phase stabilization the visibility of the setup was limited to 90%. To avoid the need to actively stabilize their setup, the authors of [13] combined the downconversion pairs created in a type-I BBO crystal on a symmetric beamsplitter in an intrinsically phase-stable Sagnac interferometer. This configuration proved to be stable, but the achieved count rates and visibilities did not come close to the configurations realized before. Finally, in a recently published work Kim et al. [14] ingeniously combined the advantageous features of [12] and [13], bidirectionally pumping a type-II PPKTP crystal in a polarization Sagnac interferometer. The authors reported a detected photon-pair yield of 5000 $(s\,mW\,nm)^{-1}$ at a 96.8% visibility. In an update [15], these numbers were significantly improved to 9800 $(s\,mW\,nm)^{-1}$ at 98% visibility.

During this time, there has also been significant improvement in the development of correlated photon-pair sources based on four-wave mixing in single-mode fibers [16, 17] and SPDC in nonlinear crystal waveguides [18]. The strong spatial confinement of the pump beam in nonlinear waveguides leads to higher effective material nonlinearities and thus the generation of photon pairs of much higher spectral brightness than in bulk periodically poled crystals. Yet, to date no high quality polarization entanglement has been demonstrated in these schemes.

In this paper we demonstrate a fiber-coupled source of polarization-entangled photons, based upon the scheme by Kim et al. [14]. We show that the wavelength of the downconversion photons can be tuned without loss of visibility over a range of ± 26 nm around degeneracy merely by changing the temperature of the nonlinear crystal. Wavelength tunability of entangled photons has been claimed before [8, 9] but was not demonstrated to the extent achieved here. The high purity of the entangled photon state in our setup enables further tests on fundamental concepts of physics for example on the violation of local or non-local realism [19, 20], which place increasingly stringent lower bounds on the required degree of entanglement. The high spectral brightness of the source makes it perfectly suitable for free-space quantum communication experiments [21–23]. Given that the range of wavelengths accessible to this source covers important atomic transitions in rubidium or caesium, it is also a promising candidate for atom-photon coupling experiments, e.g. photonic memories for quantum repeaters [24, 25].

The paper is organized as follows: in section 2 we briefly review spontaneous parametric downconversion in periodically poled crystals. In section 3 we discuss the influence of the crystal length on the performance of a downconversion setup as well as the optimal focusing conditions for type-II PPKTP crystals of varying length. In section 4 we describe the source of polarization-entangled photons and in section 5 we present our results on obtained spectral brightness, quality of entanglement and wavelength tunability.

2. Downconversion in periodically poled crystals

Parametric downconversion in a nonlinear crystal can be described by the spontaneous splitting of a pump photon (p) into a pair of photons (usually called *signal s* and *idler i*) according to conservation of photon energy $\omega_p = \omega_s + \omega_i$ and momentum. In periodically poled crystals, the effective nonlinearity of the medium is periodically inverted by the application of an electric field with alternating directions during the crystal fabrication process. In contrast to birefringent phasematching in bulk crystals the quasi-phasematching conditions now involve an additional term which depends on the crystal-poling period Λ:

$$\mathbf{k}_p(\lambda_p, n_p(\lambda_p, T)) = \mathbf{k}_s(\lambda_s, n_s(\lambda_s, T)) + \mathbf{k}_i(\lambda_i, n_i(\lambda_i, T)) + \frac{2\pi}{\Lambda(T)} \tag{1}$$

where $\mathbf{k}_{p,s,i}$ are the wavevectors of the pump, signal and idler photons, and $n_{p,s,i}$ the wavelength and temperature-dependent refractive indices of the crystal for the respective wave fields. Assuming a fixed pump wavelength, Eq. 1 shows that the $\mathbf{k}$ vectors of the signal and idler photons are temperature dependent, in particular, for a fixed emission angle, wavelength-degenerate photons will only be created at one certain temperature T. Quasi-phasematching in periodically poled crystals allows for almost arbitrary phasematching angles and wavelengths in comparison to the nontrivial conditions in bulk nonlinear crystals, where only birefringent and angle phasematching is possible. In particular, periodically poled crystals can be tailored such that $\mathbf{k}_{p,s,i}$ are parallel to one of the crystallographic axes X, Y or Z. For a type-II SPDC process this means that the orthogonal signal and idler beams do not experience transversal walkoff, an effect which severely limits the maximum useful length of birefringent nonlinear crystals to less than 10 mm in typical downconversion setups. In section 3 we compare photon-pair yields coupled to single-mode optical fibers and the corresponding single-photon bandwidths of downconversion photons created in periodically poled crystals of various lengths. Furthermore we find the optimal focusing conditions for each crystal resulting in unprecedented photon yields.

3. Optimization of beam focusing and crystal properties

In downconversion experiments it is well known that focusing the pump beam drastically improves count rates and collection efficiencies into single-mode fibers. The quest for the optimal focusing parameters has been the subject of theoretical and experimental investigations [26–28]. We followed the lines of Ljunggren et al. [28], who numerically calculated optimal focusing conditions for downconversion in PPKTP crystals and made predictions for the expected dependence of count rates and photon bandwidths on crystal length. The two key parameters for an entangled photon source which can be maximized via optimal focusing are the detected coincidence rate R_c and the coincidence-to-single-photon (coupling) ratio $\eta_c = R_c/\sqrt{R_i R_s}$, with R_i and R_s being the single photon count rates. As pointed out in [28] the focusing conditions for these parameters are not generally the same, as the number of single photons and photon pairs coupled into fibers do not solely depend on the total number of pairs created but also on the mode quality factor M^2 of the downconversion and its overlap with the fiber modes.

Here, instead of measuring M^2 factors as done in [28] we directly compared single photon and coincidence count rates for four ($L = 10, 15, 20, 25$ mm) X-cut flux-grown PPKTP crystals manufactured by *Raicol*. The crystals had a grating period of 10 μm and were quasi-phasematched for collinear degenerate downconversion at $\lambda_p = 405$ nm and $49.2\,^\circ$C. The 405 nm laser diode used in our setup had limited power, therefore we chose to find the optimal focusing conditions for a maximal coincidence rate $R_{c\,\mathrm{max}}$.

We pumped a given crystal of length L with spot waist sizes w_p from $15-55\ \mu m$, coupling the downconversion into a single-mode fiber attached to a fiber beamsplitter and two detectors. For each w_p we varied mode waist sizes $w_{s,i}$ between $(15\mu m < w_{s,i} < 55\mu m)$ and monitored $R_{s,i}$ and R_c. The obtained data, exemplary shown for the $L = 15$ mm crystal in figures 1(a) and (b), was numerically fitted with polynomial functions. From these fits, for each w_p we obtained one optimal $w_{s,i\ \text{opt}}$ and, in consequence one optimal set $(w_p, w_{s,i})_{\text{opt}}$ for each crystal length L.
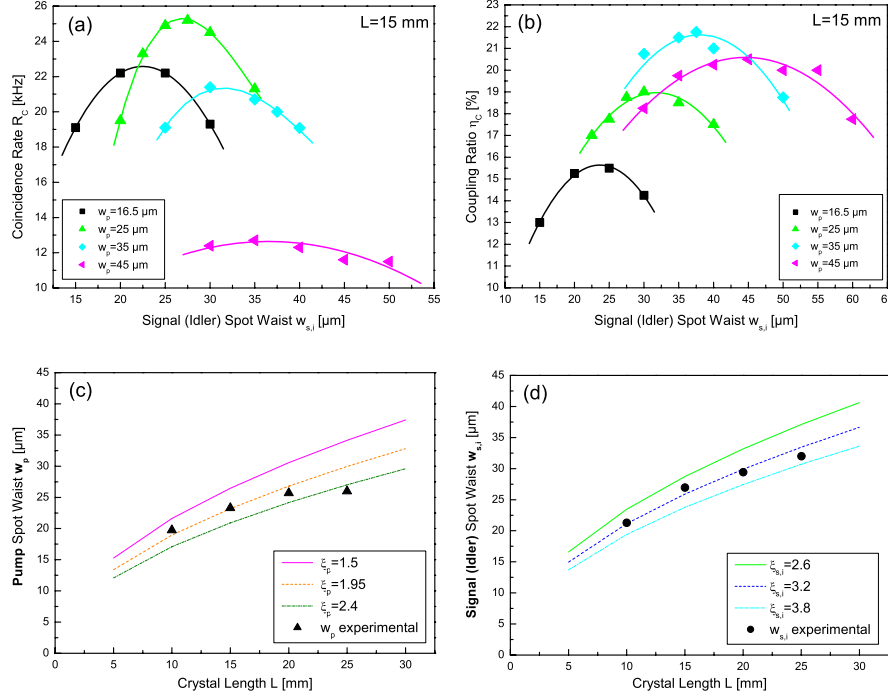
Fig. 1. Measured coincidence count rates R_c (a) and coupling ratios η_c (b) for a $L = 15$ mm crystal for a series of focusing conditions in a simple test setup (described in the text). From these measurements we determined pump (c) and signal (idler) (d) spot waist sizes w_p and $w_{s,i}$ for maximal photon-pair count rate $R_{c\ \text{max}}$ and crystals of length $10, 15, 20$ and 25 mm. The detected count rates were repeatable to within 5%. The lines drawn for three constant values of the dimensionless parameters ξ_p and $\xi_{s,i}$ ($\xi = L/z_r$, where z_r is the Rayleigh range) show the supposed independence of $\xi_{p\ \text{opt}}$ and $\xi_{s,i\ \text{opt}}$ of L. While this behavior is certainly given for $\xi_{s,i\ \text{opt}}$ (black dots), it was not observed for $\xi_{p\ \text{opt}}$. (black triangles).

The results in Fig. 1 (c) and (d) show the spot waist sizes for maximal photon-pair yield for the pump beam and the signal (idler) modes for different crystal lengths. For crystals from $10-25$ mm the optimal focusing conditions for $R_{c\ \text{max}}$ are $(20\mu m \lesssim w_{p\ \text{opt}} \lesssim 26\mu m)$ (Fig. 1(c)) and $(21\mu m \lesssim w_{s,i\ \text{opt}} \lesssim 32\mu m)$ (Fig. 1(d)). Using the dimensionless parameters $\xi_p = L/z_{r\ p}$ and $\xi_{s,i} = L/z_{r\ s,i}$, where $z_{r\ p,s,i}$ are the Rayleigh ranges of the pump and the signal (idler) modes in the crystal, this corresponds to $(1.8 \lesssim \xi_{p\ \text{opt}} \lesssim 2.6)$ and $\xi_{s,i\ \text{opt}} \sim 3.2$. We found that for the signal and idler modes the focusing parameter $\xi_{s,i\ \text{opt}}$ is independent of L (cf. [28]), but that the pump focus parameter $\xi_{p\ \text{opt}}$ rises with L, which might be due to increasing contribution of grating defects in longer crystals.

For the $L = 15$ mm crystal we could also deduce the focusing conditions for a maximal cou-

pling ratio $\eta_{c\,max} = max\,\eta_c(\xi_p, \xi_{s,i})$. The parameters ξ_p and $\xi_{s,i}$ differ significantly from those for $R_{c\,max}$ with $\xi_p \sim 0.7$ and $\xi_{s,i} \sim 1.5$. The reason is presumably that for tighter confinement of the pump field within the crystal, a higher total number of pairs is generated, which results in a higher R_c. Due to the stronger focusing these pairs will however be created in spatial longitudinal modes of increasingly higher order (cf. [28]). This leads to a decrease of the overlap between the coupling fiber modes and the downconversion mode and hence to a lower coupling ratio η_c.

Consider the properties of the power spectrum of the emitted two-photon state, obtained by using first-order perturbation theory [29]:

$$I \propto sinc^2(\frac{L}{2}\Delta k) \tag{2}$$

where Δk is the phase mismatch, $k_p - k_i - k_s - \frac{2\pi}{\Lambda}$. The authors of [28] conclude that the flux of downconversion photons R_c coupled into single-mode optical fibers in collinear configurations with optimal focusing relates to the crystal length L as

$$R_c \sim \sqrt{L}. \tag{3}$$

The $sinc^2$ function in Eq. 2 drops to a value of 0.5 for $\frac{L}{2}\Delta k = 1.39$. By writing Δk as a function of λ_i, expanding Δk in a Taylor series around $\lambda_i = 810$ nm and neglecting higher order terms, we arrive at an expression for the single-mode bandwidths of the signal and idler photons:

$$\Delta\lambda_{s,iFWHM} = \frac{5.52x10^{-3}}{L} \text{ nm} \tag{4}$$

The spectral brightness B of the produced downconversion light, a value for the comparison of different downconversion setups, given by the number of produced photon pairs per second, per milliwatt of pump power and per nm bandwidth, therefore scales as $B \sim L\sqrt{L}$.
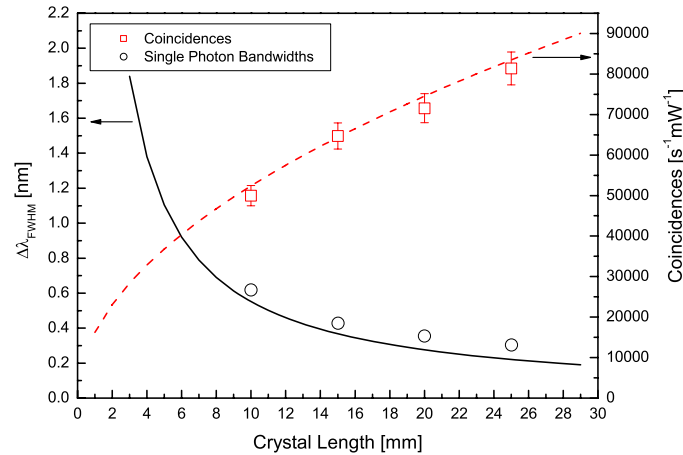

Fig. 2. Measured spectral bandwidths (FWHM) of downconversion photons and photon-pair yields for PPKTP crystals of various lengths. The single photon bandwidth (black circles) was determined via interference in a single photon Michelson interferometer and is shown compared to theoretic values calculated using Eq. 4 (black line). The measured coincidence rates (red squares) show the expected square root dependence on L (Eq. 3).

The experimental results on the photon-pair yield R_c and the bandwidth $\Delta\lambda_{s,i}$ of the down-converted photons for different crystal lengths are shown in Fig. 2. The maximum photon-pair yields R_c resulted from the evaluation of the optimal focusing conditions. A least-square fit of the corresponding data points to Eq. 3 yielded $R_c(L) = 16220 \times \sqrt{L}$ pairs $s^{-1}mm^{1/2}$ with excellent agreement to the square root dependence on L. The photon bandwidths $\Delta\lambda_{s,i}$ were determined with a single-photon Michelson interferometer and in Fig. 2 directly compared to the single-mode bandwidths predicted by theory (Eq. 4).
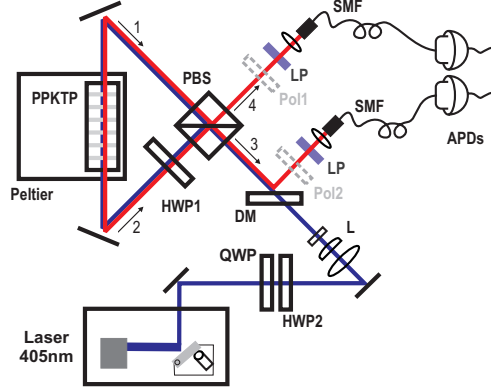
4. Entangled Photon Source Setup

Fig. 3. Scheme of the fiber-coupled entangled photon source. A 405nm *Littrow* diode laser whose polarization and phase are set by a quarter- (QWP) and a half-wave plate (HWP2) is focused via a combination of one spherical and two cylindrical lenses (L) into a PPKTP crystal inside a polarization Sagnac loop built up by dual-wavelength polarizing beamsplitter (PBS) a dual-wavelength half-wave plate (HWP1) (anti-reflection coated for 405 and 810 nm) and two laser mirrors. The downconversion modes are coupled into single-mode fibers (SMF). Remaining stray laser light is blocked by two RG715 longpass color glass filters (LP). Polarizers (Pol1, Pol2) can be inserted to characterize the produced photon pairs.

Once we had found the optimal focusing conditions for the PPKTP crystals and ascertained that the use of long crystals indeed yielded more photon pairs and narrower bandwidth, the entangled photon source was set up. The source is pumped by a *Toptica* 405 nm grating-stabilized laser diode, focused to a circular spot of waist $w_o = 27 \, \mu m$ at the center of the crystal. The polarization state of the laser beam is controlled by a combination of a halfwave- (HWP2) and a quarter-wave plate (QWP). The 25 mm PPKTP crystal is mounted in a crystal oven, at the center of a polarization Sagnac interferometer (PSI) which consists of a dual wavelength polarizing beamsplitter cube (PBS), a dual wavelength half-wave plate (HWP1) oriented at $\frac{\pi}{4}$ and two laser mirrors (see Fig. 3). The vertical component of the laser beam is reflected at the PBS and rotated to horizontal orientation by HWP1. It creates pairs of photons with orthogonal polarizations $|H_s\rangle_1$ and $|V_i\rangle_1$, the number subscripts denoting the spatial mode of the photons, which propagate in clockwise direction. The horizontal component of the beam is transmitted at the PBS and likewise creates pairs $|H_s\rangle_2$ and $|V_i\rangle_2$ propagating in counterclockwise direction. At HWP1, $|H_s\rangle_2$ and $|V_i\rangle_2$ are rotated by $\frac{\pi}{2}$ into $|V_s\rangle_2$ and $|H_i\rangle_2$. The counterpropagating pairs in modes 1 and 2 are then combined at the PBS, where again horizontal photons are transmitted and vertical photons reflected such that $|H_s\rangle_1, |V_i\rangle_1 \rightarrow |H_s\rangle_3, |V_i\rangle_4$ and $|V_s\rangle_2, |H_i\rangle_2 \rightarrow |V_s\rangle_3, |H_i\rangle_4$. The two-photon state emerging in modes 3 and 4 is thus $|H_s\rangle_3 |V_i\rangle_4 + e^{i\phi} |V_s\rangle_3 |H_i\rangle_4$. The phase ϕ

is set via appropriate adjustment of HWP2 and QWP [14]. Output mode 3 is identical to the pump input mode, therefore the downconversion photons have to be separated from the pump by a dichroic mirror (DM). Subsequently, the photons in modes 3 and 4 are coupled into single-mode optical fibers whose waists are matched via $f = 18.4$ mm aspheric lenses to the pump waist in the crystal according to the focus parameters given in section 3. Since the single-mode fibers are spatial mode filters for the downconversion light, there is no need for additional lossy interference filters as in [14].

Note that, due to birefringence, orthogonally polarized photons in the crystal travel at different group velocities, causing the $|H\rangle$ photon to leave the crystal before the $|V\rangle$ photon. This longitudinal walkoff renders the photons partly distinguishable and leads to a decrease in the degree of entanglement. This effect, which is inherent to all Type-II downconversion schemes, is compensated by flipping the two photons in the counterclockwise arm of the PSI by $\frac{\pi}{2}$. The longitudinal walkoff of pair 2 is inverted with respect to pair 1 and while there is still always a non-zero delay between $|H\rangle$ and $|V\rangle$ photons in modes 3 and 4, the arrival time of the photons contains no information about the respective photon polarization anymore. The efficiency of this compensation scheme depends only on the precision and orientation of HWP1 and is thus more effective than in other schemes [6].

5. Entangled photon source performance and tunability

The use of a 25 mm long PPKTP crystal in the perfectly compensated PSI scheme and the optimum choice of focus parameters results in unprecedented photon yields, spectral brightness and a very high degree of entanglement. Using a *PerkinElmer* SPCM-AQ4C single photon detector array with a quantum efficiency of $\sim 40\%$ and a home-built FPGA coincidence counter with a coincidence time window of 4.4 ns, we detected 82000 photon pairs/s at 1 mW of pump power.
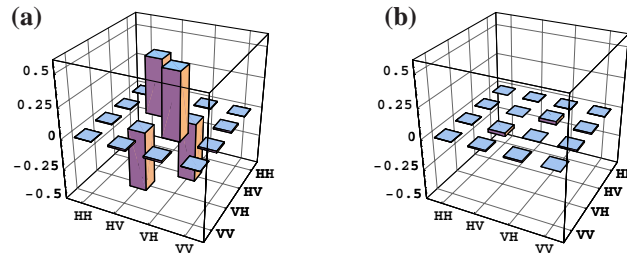

Fig. 4. (color online) Tomography of the two-photon quantum state. The real (a) and imaginary (b) part of the density matrix was reconstructed from 36 linearly independent coincidence measurements. The resulting fidelity F to the $|\psi^-\rangle$ state was $F = 0.9959 \pm 0.0001$ and the Tangle $T = 0.9875 \pm 0.0003$. Within the resolution of this representation the experimental graph is in excellent agreement to the theoretic expectation.

The overall transmission of the optical components in the setup including the single-mode fibers, which were not AR-coated, and the $100 : 1$ extinction ratio of the PBS, averaged over the optical paths for output mode 3 and 4 amounts to 84.6%. Combined with the detector efficiency, the maximal achievable coupling ratio η_c^0 is therefore 33.8%. The actually observed η_c was 28.5%. This shows that in our setup the mode overlap η_c/η_c^0, i.e. the probability that one photon of a pair is collected given that its partner photon is in its respective collection mode, is 84.3%. When set to the optimal focusing conditions for $\eta_{c\,max}$, the photon pair yield

of the source decreases by 20% to 65000 pairs/s while the mode overlap increases to 95%, to our knowledge the highest value reported so far.

The photons have a measured $FWHM$ bandwidth of 0.3 nm (see Fig. 2), the spectral brightness of the source is therefore 273000 pairs $(\text{s mW nm})^{-1}$. The visibility of the two-photon quantum state measured for degenerate photons ($\lambda_{s,i} = 810$ nm) in the $|\pm\rangle = \frac{1}{\sqrt{2}}(|H\rangle \pm |V\rangle)$ basis was 99.5%. The produced entangled state was further characterized using full quantum state tomography [30]. The fidelity $F = \langle \psi^- | \rho | \psi^- \rangle$ of the two-photon density matrix ρ with the maximally entangled state $|\psi^-\rangle = \frac{1}{\sqrt{2}}(|H\rangle |V\rangle - |V\rangle |H\rangle)$ was $F = 0.9959 \pm 0.0001$ and the tangle, a measure for the degree of entanglement as defined in [31] was $T = 0.9875 \pm 0.0003$. The measurements for visibility and quantum state tomography were performed at 0.25 mW of pump power and averaged over 10 seconds. The statistical standard deviations of these results were estimated by performing a 100 run Monte Carlo simulation of the state tomography analysis, with Poissonian noise added to the count statistics in each run [30]. Figure 4 shows the reconstructed real and imaginary parts of the density matrix ρ of the produced states. After subtraction of accidental coincidences caused by detector darkcounts, fidelity and tangle increase to $F = 0.9978 \pm 0.0001$ and $T = 0.9940 \pm 0.0001$, respectively. The state is thus very close to a pure entangled state. Indeed in the H/V basis we measured polarization contrasts of up to 9500:1 (accidentals subtracted), a regime where visibility measurements are limited by the extinction ratio of the polarizers, which was found to be $10000 : 1$.
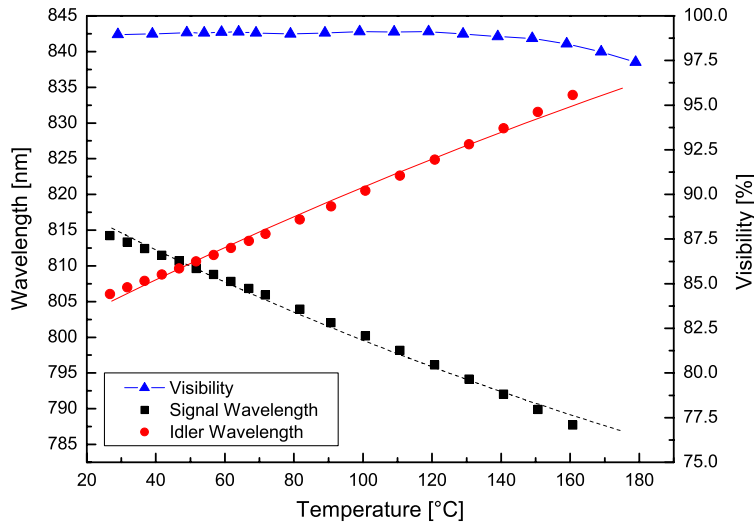

Fig. 5. Signal (black rectangles) and idler (red circles) wavelengths and 2-photon visibility (blue triangles) as a function of crystal temperature. The wavelengths were measured with a scanning single photon spectrometer with a resolution of 0.2 nm. Our crystal oven allows us to reach a wavelength spacing of more than 50 nm.

The exact crystal temperature for wavelength degeneracy, 49.2 °C, was calculated from theory via Eq. 1. We experimentally confirmed this temperature with a single-photon spectrometer, measuring λ_i and λ_s for temperatures from 25 °C to 60 °C (see Fig. 5). The most striking feature of the setup is that the visibility of the entangled state stays above 99% in a large wavelength range (Fig. 5). It starts to decrease slightly for wavelength shifts of more than ± 18 nm, reaching 97.5% at 810 ± 26 nm at ~ 180 °C. The most likely cause for this decrease is that all optical components in the setup were specified and coated for 810 nm and act as

partial polarizers at substantially higher or lower wavelengths. The refractive indices needed to calculate theoretical values for λ_i and λ_s, according to Eq. 1, were obtained via the Sellmeier and temperature-dependent Sellmeier equations for KTP from [32] and [33]. The thermal expansion coefficient for KTP which affects the crystal poling period Λ also stems from [33]. Note that these equations are of an empirical nature and do not exactly reproduce the actual refractive indices for the whole spectral and temperature range. In particular, the temperature-dependent extensions for the Sellmeier equations from [33] do not extend to wavelengths lower than 532 nm. In order to reproduce the crystal temperature for degenerate downconversion and to obtain an accurate wavelength fit over the whole temperature range, we had to adopt $\partial n_y / \partial t \mid_{405nm} = 28 \times 10^{-6}$, reported in [34].

6. Conclusion

We have demonstrated a fiber-coupled, wavelength-tunable source of narrowband, polarization-entangled photons. By comprehensive optimization of focusing conditions and the use of a 25 mm long crystal, we achieved a spectral brightness of 273000 (s mW nm) $^{-1}$, a factor of 28 higher than comparable previous setups. The entangled state has a tangle $T = 0.987$ and the coupling ratio is 28.5%. We demonstrated wavelength tuning of entangled photons in a range of ± 26 nm around degeneracy with virtually no decrease in entanglement. These properties, combined with the intrinsic phase stability of the Sagnac-type setup, the compactness, and the ease of use, make this setup a perfect tool for quantum communication experiments both in the laboratory and in the field.

Acknowledgements